TRACE CHEMICAL VAPOR DETECTION BY PHOTOTHERMAL INTERFEROMETRY

Paul M. Pellegrino, Nicholas F. Fell, Jr., Scott D. Sarama, and James B. Gillespie
U.S. Army Research Laboratory, 2800 Powder Mill Road,
Adelphi, Maryland 20783-1197

ABSTRACT

Photothermal interferometry has been demonstrated for detection of vapors with extremely high sensitivity (parts-per-trillion). Our present research uses a photothermal detection scheme that incorporates tunable sources and a modified Jamin interferometric design to provide high selectivity and sensitivity for organo-phosphate vapor detection. Phase shifts on microradian levels have been detected. Trace chemical vapor detection is accomplished by introducing the tunable excitation laser along the path of one interferometer beam providing a phase shift due to absorptive heating. Preliminary results indicated parts-per-billion detection of both DMMP and DIMP using ~400mW of CO_2 laser power at appropriate wavelengths.

INTRODUCTION

Monitoring trace gases in our environment has many actual and potential uses. Escalating environmental awareness has led to more restrictive regulations on air quality in both the workplace and environment in general. Both industry and the military have expressed interest in development of more sensitive and adaptable trace gas analysis instrumentation. After the Tokyo subway sarin attack, the detection of CW agents became a crucial area of research in both the civilian and military arenas. Since many CW agents have low vapor pressures and are quite toxic, detection limits in the ng/mL range are required for fieldable systems. This detection limit highlights the need for extremely sensitive devices and techniques. A more general environmental application of trace gas detection can be seen in workplace monitoring for specific pollutants. An important example involves the detection of monomethylhydrazine (MMH) and unsymmetrical dimethylhydrazine (UDMH). These materials are common components in certain types of rocket fuel as well as etchants in microstructure fabrication. Typical National Institute for Occupational Safety and Health (NIOSH) exposure levels are 30-60 parts-per-billion (ppb)[1] depending on the form of the hydrazine. This example also demonstrates that the degree of sensitivity needed in certain circumstances can exceed the limits of detection for common monitoring systems.

Photothermal spectroscopy encompasses a group of highly sensitive methods that can be used to detect trace levels of gases using optical absorption and subsequent thermal perturbations of the gases. The underlying principle that connects these various spectroscopic methods is the measurement of changes in physical parameters (temperature, pressure, or density) as a result of photo-induced change in the thermal state of the sample. Photothermal methods in general are classified as indirect methods for detection of trace optical absorbance, because the transmission of the light used to excite the sample is not measured directly. Several

Report Documentation Page

Form Approved
OMB No. 0704-0188

1. REPORT DATE	2. REPORT TYPE	3. DATES COVERED
00 JAN 2002	**N/A**	**-**

4. TITLE AND SUBTITLE	5a. CONTRACT NUMBER
Trace Chemical Vapor Detection By Photothermal Interferometry	5b. GRANT NUMBER
	5c. PROGRAM ELEMENT NUMBER
6. AUTHOR(S)	5d. PROJECT NUMBER
	5e. TASK NUMBER
	5f. WORK UNIT NUMBER
7. PERFORMING ORGANIZATION NAME(S) AND ADDRESS(ES) **U.S. Army Research Laboratory, 2800 Powder Mill Road, Adelphi, Maryland 20783-1197**	8. PERFORMING ORGANIZATION REPORT NUMBER
9. SPONSORING/MONITORING AGENCY NAME(S) AND ADDRESS(ES)	10. SPONSOR/MONITOR'S ACRONYM(S)
	11. SPONSOR/MONITOR'S REPORT NUMBER(S)

12. DISTRIBUTION/AVAILABILITY STATEMENT
Approved for public release, distribution unlimited

13. SUPPLEMENTARY NOTES
This article is from ADA409494 Proceedings of the 2001 ECBC Scientific Conference on Chemical and Biological Defense Research, 6-8 March , Marriott's Hunt Valley Inn, Hunt Valley, MD., The original document contains color images.

14. ABSTRACT

15. SUBJECT TERMS

16. SECURITY CLASSIFICATION OF:			17. LIMITATION OF ABSTRACT	18. NUMBER OF PAGES	19a. NAME OF RESPONSIBLE PERSON
a. REPORT	b. ABSTRACT	c. THIS PAGE			
unclassified	**unclassified**	**unclassified**	**UU**	**8**	

examples of these techniques include photoacoustic spectroscopy (PAS), photothermal lensing (PTL), photothermal deflection (PTD), and photothermal interferometry (PTI). In PAS the pressure wave produced by the sample heating is measured, while the other examples sense the refractive index directly changes in the refractive index or by use of combinations of probe sources and detectors. The photothermal method we have chosen to pursue is photothermal interferometry. Recent research suggests that trace gas detection at parts-per-trillion (pptr) levels is attainable with this photothermal technique.[2,3]

In the late 1960's it was recognized that optical absorption resulting in sample heating and subsequent changes in the index of refraction would induce a phase shift in light probing the heated region. McLean, Sica, and Glass[4] were the first to demonstrate use of an interferometer to measure these photo-induced index changes. Most PTI apparatus are based on laser sources for both excitation and probe. Later Stone[5,6] incorporated both coherent and incoherent excitation sources in a modified Jamin interferometer to measure trace absorption in liquid samples. Other notable contributions to PTI include measurements by Davis and Petuchowski,[7] who achieved a lower detection limit of the infrared absorption coefficient of 10^{-10} cm^{-1} for a gaseous sample in a windowless cell. Recent research by Owens *et.al.*[2] demonstrated atmospheric ammonia detection at pptr levels using an apparatus similar to the Davis designs[7]. The literature indicates that a trace gas sensor with high sensitivity can be constructed using interferometer designs similar to ones previously mentioned.[1-4,7,8]

We have designed, built, and are testing a new instrument for trace gas analysis in ambient air by PTI. The design uses a Jamin interferometer with a specialized optical coating, mid-IR excitation source, and HeNe probe source. Initial tests have established the ability to detect trace levels of two methylphosphonate compounds with modest amounts of CO_2 laser power. Methylphosphonates are well-studied simulants for nerve agents and pesticides. Our goals are to develop a PTI system with the ability to not only detect trace gases, but also to discriminate target gases from the normal atmospheric backgrounds and each other. Our work targets CW agent simulants to demonstrate the capabilities of PTI in this area. We have initially characterized the system performance with a waveguide CO_2 laser. We have also examined difference frequency generation (DFG) as a possible method for generating tunable light in the 8-12 μm region. The first literature demonstrating DFG as a tunable mid-IR source (2.2-4.2 μm) using CW laser was report by Pine in the mid-1970's[9]. Recent literature involving tunable diode lasers with and without amplifers have established this a possible foundation for a widely tunable infrared source[10-12]. Frequency agile sources such as DFG sources are of particular interest as they increase discrimination ability by providing absorbance information as a function of wavelength. A description of our DFG experiment will be given along with preliminary results.

THEORY

PHOTOTHERMAL THEORY

In this section the underlying physical principles of PTI will be described in relation to our experimental system. Since PTI relies on detection of phase shifts produced by photo-induced heating of a sample, having excitation sources that overlap the peaks in the absorption spectrum of analyte gases is extremely important. Also, focusing on wavelengths that provide unique spectral information about the sample strengthens the capabilities of the sensor. Due to these considerations we have chosen to probe the optical absorbance in the mid-infrared spectral region (8-12 μm). This region offers a wealth of information about the chemical structure of the CW agent simulants being investigated. A typical infrared absorption cross-section for one of these molecules, dimethyl methylphosphonate (DMMP), s_{DMMP}, is approximately 44 atm^{-1} cm^{-1} near the 9P(26) CO_2 laser line. These large absorption cross-sections make the molecule well suited to absorption of the mid-infrared pump laser and subsequently convert the energy that is not re-emitted to heat after molecular relaxation, primarily through collisional relaxation. The collisional relaxation that occurs causes a temperature increase in the sampled gas according to,

$$\Delta T = \frac{PsN}{2frC_p pa^2}, \qquad (1)$$

where P is the IR excitation power, f is the laser modulation, r and C_p are the density and heat capacity of the sampled gas, respectively, N is the molecular number density, and a is the IR laser beam radius. The rate of relaxation of the organophosphonate analytes studied can be estimated to be in the sub-nanosecond region using general gaseous thermodynamic equations[13]. The conduction of the heated air in our sample is slow relative to the relaxation time for organophosphonate samples, and the displacement due to convection of the heated gas is small compared to the radius of the laser probe beam. This implies that we can regard the heating of the gas from the excitation source to be both instantaneous and localized within the probe beam. Modulation frequencies are chosen by considering both noise levels and the frequency dependence of the temperature change, as seen in equation (1). Given the quasi-static local heating in the probe beam, the modulated index of refraction change follows the Clausius-Mossotti equation and is given by,

$$\Delta n = -(n-1)\Delta T / T_{abs}, \tag{2}$$

where T_{abs} is the absolute temperature of the gas. The modulated index of refraction induces a modulated phase shift,

$$f_m = 2pl\Delta n / l, \tag{3}$$

in the HeNe probe beam in one arm of the interferometer where l is the interaction path length, and l is the wavelength of the interferometer laser. The complementary outputs of the interferometer are detected on two photodiodes. The difference in the intensities of the photodiode outputs is isolated by an instrumentation amplifier and the difference signal is sent to both the computer and a phase sensitive lock-in amplifier. The signal, S, is proportional to Δf_m, the difference between the complementary outputs of the interferometer, and is given by,

$$S = G\sin(\Delta f_m) = G(\Delta f_m), \tag{4}$$

with the final expression valid only for small Δf_m. The interferometer amplification factor, G, is a measure of the total system amplification.

DFG THEORY.

A brief description of the general principles underlying the theory involved in DFG will be discussed. Formal and more complete descriptions of the technique can be found in numerous texts and journal publications[10,14]. The basic process relies on the second-order nonlinear susceptibility $c^{(2)}$, which is normally associated with a limited number of nonlinear crystal types. The two higher frequency photons (w_1, w_2) enter the material and interact with the nonlinear polarizability of the crystal creating a photon at a lower frequency (w_3) corresponding to the energy difference of the two input photons. Conditions regarding conservation of energy, momentum or phase matching, and transparency at all wavelengths must be meet. The phase matching method employed in our DFG technique uses the natural birefringence of the crystal and anglular orientation with respect to the optic axis to ensure matching of the wave vector constraints ($\boldsymbol{Dk = 0 = k_1 - k_2 - k_3}$). The infrared power generated , P_3 ,in our mixing experiments can be approximated by the following equation,

$$P_3 = \frac{(32pw_3 c_{15}^{(2)})^2}{n_1 n_2 n_3 c^3} P_1 P_2 \left\{ l^2 / (w_1^2 + w_2^2) \right\}, \tag{5}$$

derived by Boyd and Ashkin in the near-field case[15]. Where P_i , n_i , w_i (i=1,2,3) are the power, refractive index and beam radius respectively and l is the crystal length described in equation 5. Initially, theoretical calculations using this equation to generate 10 μm infrared radiation yielded power estimates of 627 nW.

EXPERIMENTAL

PHOTOTHERMAL EXPERIMENTAL APPARATUS

The block diagram of the PTI beam paths and supporting analysis equipment is shown in Figure1. The border in the diagram corresponds to an acrylic enclosure that surrounds the interferometer portion of the system. This section also rests on a 2.5-inch thick optical honeycomb board. The beam from a stabilized HeNe laser (Spectra-Physics model 117A), the probe beam, is initially directed to a steering mirror before entering the first of two specially coated etalons. The etalons have anti-reflection (AR) coatings on the front surfaces except for a centered 50/50 beamsplitting (BS) stripe while the back surfaces have high-reflection coatings. All coatings are designed for the HeNe wavelength (632.8 nm) and S polarizations. The probe beam initially enters the first etalon, is reflected off the back surface, and is subsequently split by the BS stripe. One beam exits the optic while the other beam undergoes a second reflection off the back surface before exiting. Thus, the output of the first etalon is two equal intensity beams separated by ~12 mm edge to edge. These beams define the two interferometer arms and travel through an open-ended acrylic tube (32 cm long) en route to an identical second etalon 60 cm away. The second etalon acts to recombine equal amounts of both interferometer arms into two complementary outputs of the interferometer. The modified-Jamin interferometer design gives the system superior rejection of mechanically induced noise due to the common optical path of both arms and the lack of moving parts. The complimentary outputs are detected by two photodiodes (United Detector Technologies PIN 10DP). The signals are passed into a custom-fabricated instrumentation amplifier that provides the difference signal to both the lock-in amplifier (Stanford Research Systems SR510) and a personal computer running a LabVIEW (National Instruments) control program. The control program accepts inputs from the lock-in amplifier, instrumentation amplifier, and the power meter. A 1-second average of the DC component of the

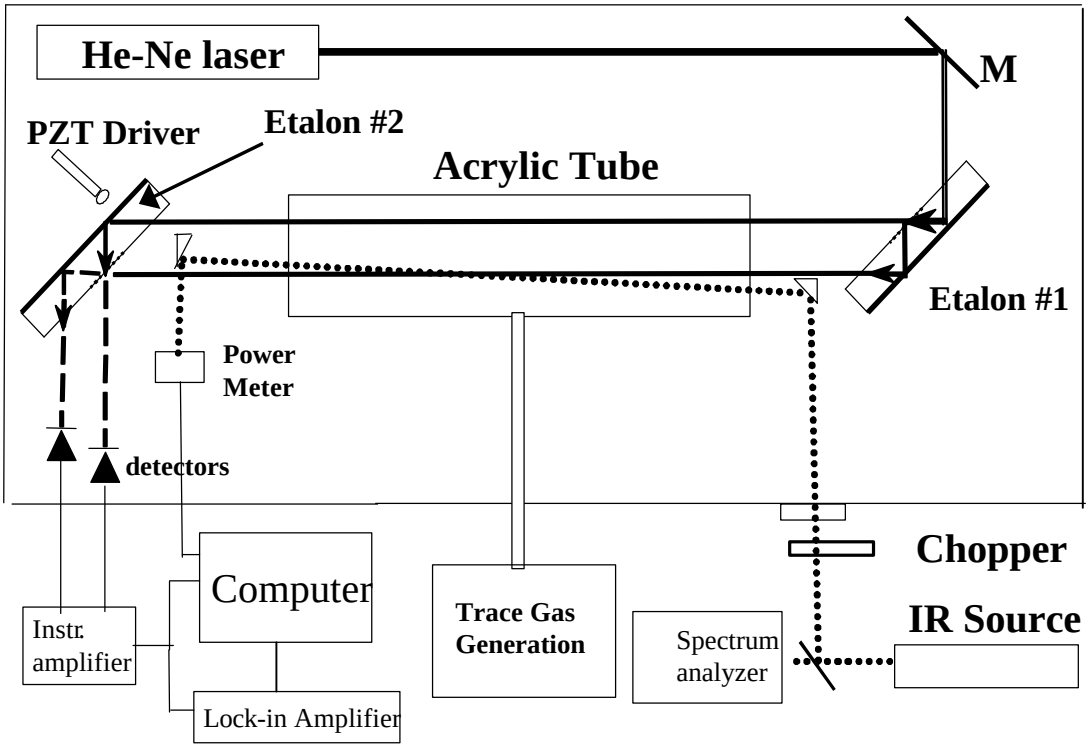

Figure 1. Experimental block diagram for modified-Jamin photothermal interferometer.

difference signal is used for feedback to control the piezo-electric (PZT)driven micrometer on the second etalon. This feedback control is used to maintain the interferometer in a quadrature position, which is the most sensitive position in relation to changes in the phase shift and the center of the linear response range. The lock-in signal and the measured IR power are used to provide an excitation power normalized signal. Pure trace gases are introduced into the acrylic tube via a trace gas generator (VICI-Metronics Dynacalibrator Model 190). The gas generator is set at 100°C and pure nitrogen flows of 0.1-1.0 L/min will produce trace levels of organo-phosphate from approximately 10 ppb – 1.0 ppm depending on the length of the permeation tube in the device and the flow. The IR excitation beam is introduced from a waveguide CO_2 laser (California Laser, circa. 1984) set at wavelengths corresponding to sizeable vapor absorption cross-sections. The beam is initially split with one part entering a spectrum analyzer (Optical Engineering 16A) to provide wavelength information. The other part is modulated by a chopper (f = 600 Hz) before entering the enclosure through an AR coated ZnSe window. This beam glances off the gold-coated hypotenuse of a prism making a shallow crossing angle with one arm of the interferometer. Using another coated prism, the beam is directed to broadband power meter. The effective path length is estimated at 10 cm with the IR beam diameter of 3-4 mm, with a probe beam diameter not exceeding 2 mm. This mismatch in beam diameters can be attributed to poor beam quality of the waveguide CO_2 laser. This is not an inherent quality of these types of lasers, but is related to the age of our laser system. The mismatch prevents the efficient use all of our IR excitation power.

DFG EXPERIMENTAL APPARATUS

Figure 2 is a block diagram of the DFG configuration used in our experiment. The output of a 852 nm distributed Bragg reflector (DBR) diode laser SDL-5722 and a tunable external cavity diode laser (ECDL) SDL-TC10-1393 operating in the 910-950 nm region for type II phase matching in $AgGaS_2$ were overlapped using a dichroic beamcombiner. The beams were focused using two cylindrical lenses and an aspheric lens for the ECDL and DRB lasers respectively. The 20-cm long AR coated nonlinear crystal was mounted on a on a motorized rotation stage to allow for angle tuning of the crystal to appropriately phase match the pump wavelengths. Calculations using published Selmier data[16] indicated a tuning range of 8-12 μm was possible by tuning the crystal approximately +/- 3 degrees from normal assuming a crystal cut of 44.15 degrees with respect to the optic axis. The infrared radiation generated in the nonlinear crystal was collected by a ZnSe lens and detected with a liquid-N_2-cooled HgCdTe detector (Electro-Optics Systems MCT012) after passing through a germanium plate and optical chopper.

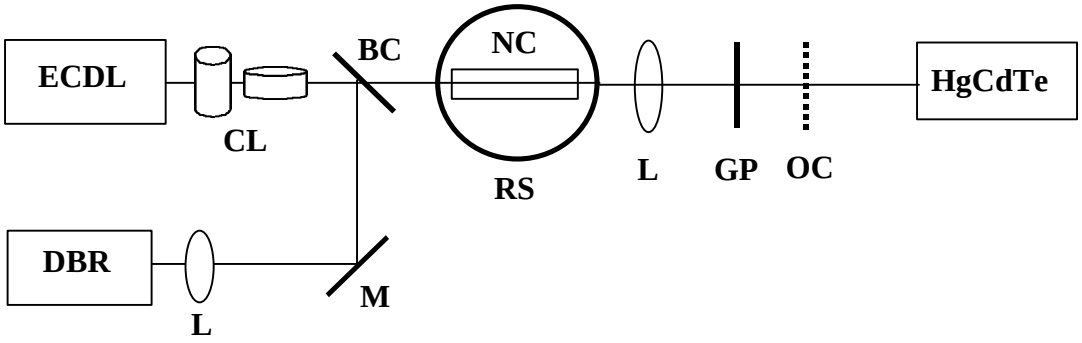

Figure 2. Block diagram of the difference frequency generation experimental set-up. L – lens, CL – cylindrical lens, M – mirror, BC – beam combiner, NC - nonlinear crystal, RS – rotation stage, GP – germanium plate, OC – optical chopper.

RESULTS AND DISSCUSSION

PHOTOTHERMAL

Initial trials were conducted by spiking the entire acrylic enclosure with minute volumes of methanol and methanol-glycerin mixtures. Using the methanol percentage, and known volumes of both the enclosure (169 L) and liquid, a partial pressure could be calculated. Figure 3 resulted from an 18-μL spike of pure methanol, which corresponds to 63 ppm partial pressure. The smooth line is a gaseous FTIR spectrum (EPA Public Gas Phase Database) overlaid on the experimental data taken with the PTI system. Despite gaps associated with the CO_2 laser this demonstrates the ability of the system to perform limited spectral discrimination using multiple lines of the grating-tuned CO_2 laser. Using methanol-glycerin mixtures and any of the 10P or 10R CO_2 lines as excitation, 1-ppm methanol levels were easily detected. Following these initial studies all beams were enclosed by the acrylic tube seen in Figure 1 and the trace gas generator was used to investigate responses from two organophosphonate compounds. Both dimethyl methylphosphonate (DMMP) and diisopropyl methylphosphonate (DIMP) permeation tubes of varying lengths were loaded in the generator. The tube lengths and calibrated flow range of our generation system limited the concentrations available for study to 10 ppb to 1 ppm. The power-corrected signal versus concentration is shown in Figure 4 for DMMP (s_{DMMP}~ 44 $atm^{-1}cm^{-1}$) excited with the 9P(26) line (P = 575 mW). The log-log plot shows excellent linearity

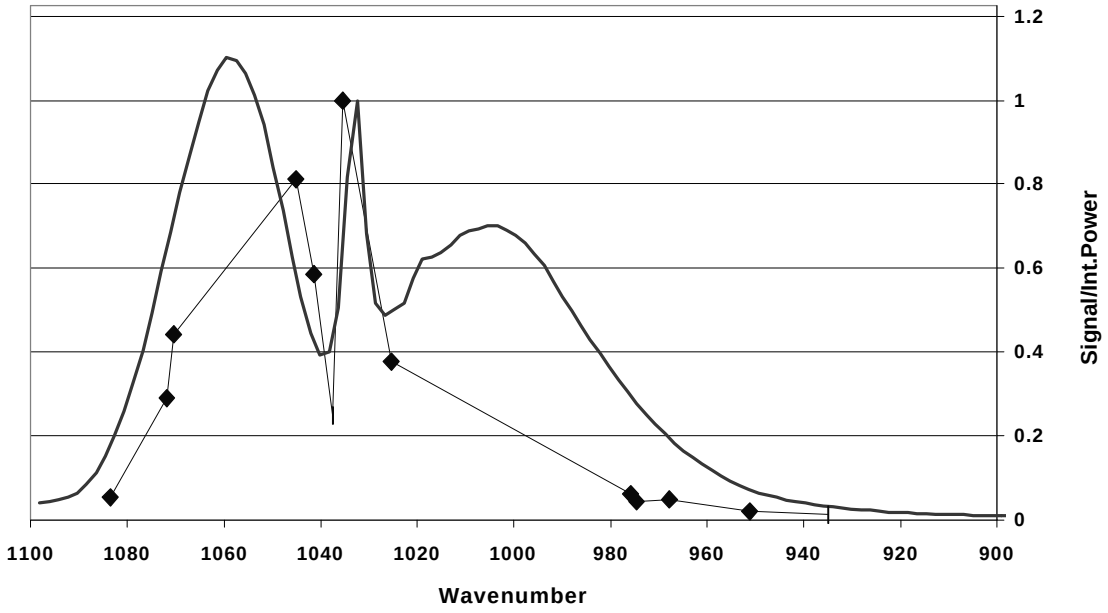

Figure 3. Spectrum of pure methanol excited with multiple CO_2 laser lines. The approximate concentration of the methanol is 63 ppm.

with a linear correlation coefficient (R^2) of 0.9987. The second organophosphonate studied provided more of a challenge to our system, due to the lack of available CO_2 lines at the maximum of the DIMP IR absorption spectrum. The DIMP absorption cross-section (s_{DIMP}~ 27 $atm^{-1}cm^{-1}$) at the 10R(32) line is substantially weaker than the DMMP peak absorption, but was still measurable. The corrected signal versus concentration is shown in Figure 4 for DIMP excited with the 10R(32) line (P = 400mW). The log-log plot of the signal shows very good linearity with an R^2 of 0.9878.

The dynamic range of our trace gas generator and the PTI system noise floor dictate the limit of our measurements on both phosphonates. The electronic noise floor of 5-7 $\mu V/(Hz)^{-1/2}$ is still excessive considering the amplifier gains on the order of 10^4 V/A. This noise level is a factor of 60 above the shot noise limit of 10^{-7} $V/(Hz)^{-1/2}$ based on the systems standard parameters. Using an alternate amplified detector set (Thor Labs

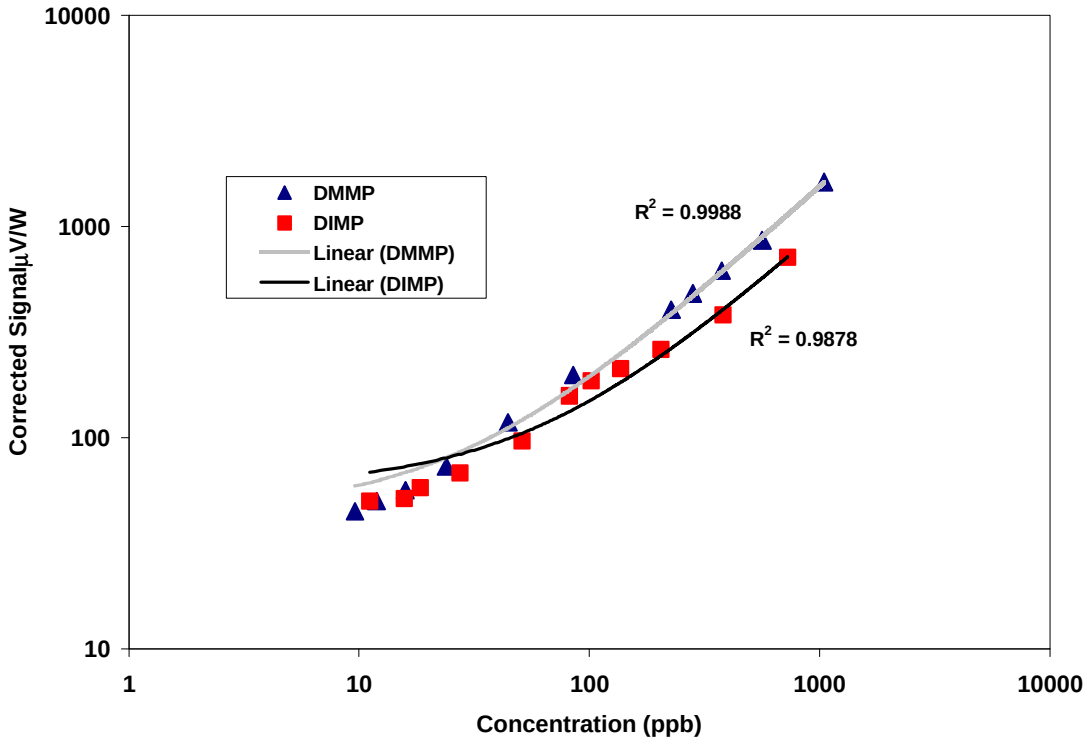

Figure 4. Log-log plot of corrected PTI signal versus DIMP and DMMP concentration.

PDA55) a calibration of the system phase sensitivity has been made. The calibration requires measurement of the interferometer as a function of PZT step, PZT step to applied voltage conversion, and finally known applied voltage to PZT drive input. Measurements were made piece-wise first recording interferometer response versus PZT step without active feedback followed by measurements of system response after known modulation was applied to PZT at normal detection frequencies. Using PZT step to applied voltage conversion factor and noise measurements the approximate phase sensitivity was calculated to be 1.85 μrad. Recent literature suggests that we can attain levels of noise that are factors of 3 to 4 above shot noise limits[3]. Other noise sources (acoustical and thermal) would probably prevent full realization of the shot noise limit. The second area that requires work is the CO_2 beam size and the shallow angle overlap. The CO_2 size should be less than or equal to the size of the probe beam to maximize use of the power that enters the interaction path. Insertion of an IR telescope to reduce the size and collimate the laser beam should make the system more efficient and aid in the alignment of the crossing.

DIFFERENCE FREQUENCY GENERATION

Result of our DFG ongoing effort to generate tunable infrared light as a source for PTI is described. Initial examination of ECDL beam showed astigmatism, which necessitated the use of two cylindrical lens to ensure co-located focusing of both vertical and horizontal directions. Use of two lens and beam combiner prior to the nonlinear crystal resulted in a beam radius that was approximately twice the optimal focus. Since the infrared output has a second-order dependence in the denominator of equation 5, the non-optimal focusing is results in an expected output that is reduced by a factor of 4. Initial attempts were centered on generation of an infrared output at 9.2 μm, which corresponds to normal incidence on a $AgGaS_2$ cut at 44.15 degrees. These attempts did not produce any measurable signal. Subsequent analysis with a version of equation 5 that includes

the walk-off term for critical (angular) phase matching[10] indicated the walk-off of our input beams could be sizeable. The walk-off of $AgGaS_2$ for our system was estimated at 22.7 mrad giving us an l_{eff} of approximately 4 millimeters. This reduced the effective length of the crystal to 20% of the total length. Conservative estimates with this effective length result in an experimentally realizable infrared output at 10-15 nW at a wavelength of 10 μm.

CONCLUSIONS

We have demonstrated the ability to detect trace amounts of organophosphonate vapor using PTI. This work focused on testing our detection system by incorporating a waveguide CO_2 as the excitation source. The measurement limits of 10 ppb for phosphonate vapors agree with the predicted sensitivity of several microradians of phase shift. Improvements on the system can be made in several key areas such as electronics and beam overlap. Initial studies on DFG for a highly tunable infrared source were performed. Experimental investigation suggests that the theoretical predictions were initially overestimated. Future work will concentrate on system improvements and continued study of difference-frequency-generation as highly tunable infrared source.

REFERENCES

1. D.L. Mazzoni and C.C. Davis, "Trace detection of hydrazines by optical homodyne interferometry," Appl. Opt. **30**, pp. 756-764, 1991.
2. M.A. Owens, C.C. Davis, and R.R. Dickerson, "A photothermal interferometer for gas-phase ammonia detection," Anal. Chem. **71**, pp. 1391-1399, 1999.
3. M.A. Owens, *Detection of Gas-Phase Ammonia Using Photothermal Interferometry*, University of Maryland, 1995 (dissertation).
4. E.A. McLean, L. Sica, and A.J. Glass, J. Appl. Phys. Lett. **13**, pp. 369, 1968
5. J. Stone, "Measurements of the absorption of light in low-loss liquids," J. Opt. Soc. Am. **62**, pp. 327-333, 1972.
6. J. Stone, Appl. Opt. **12**, pp. 1828, 1973.
7. C. C. Davis and S.J. Petuchowski, "Phase fluctuation optical heterodyne spectroscopy of gases," Appl. Opt. **20**, pp. 2539-2554, 1981.
8. S.E. Bialkowski, "Photothermal Spectroscopy Methods for Chemical Analysis," from *Chemical Analysis: A series of Monographs on Analytical Chemistry and Its Applications*, J.D. Wineforder, editor, Vol. 134, John Wiley & Sons, Inc., New York, 1996.
9. A.S. Pine, "Doppler-limited molecular spectroscopy by difference-frequency mixing," JOSA **64**, pp. 1683-1690, 1974.
10. U. Simon, Z. Benko, M. W. Sigrist, R. F. Curl, and F. K. Tittel, "Design considerations of an infrared spectrometer based on dfference-frequency generation in $AgGaSe_2$," Appl. Opt. **32**, pp. 6650-6655, 1993.
11. U. Simon, C. E. Miller, C. C. Bradley, R. G. Hulet, R. F. Curl, and F. K. Tittel, "Dfference-frequency generation in $AgGaS_2$ by use of single-mode diode-laser sources" Opt. Lett. **18**, pp. 1062-1064, 1993.
12. W. C. Eckhoff, R. S. Putnam, S. Wang, R. F. Curl, and F. K. Tittel, "A continuously tunable long-wavelength cw IR source for high resolution spectroscopy and trace-gas detection," Appl. Phys. B **63**, pp. 437-441, 1996.
13. F. Reif, *Fundamentals of Statistical and Thermal Physics*, Chapter 12, McGraw-Hill, New York, 1965.
14. R. W. Boyd, "*Nonlinear Optics*," Academic Press, New York, 1992.
15. G.D. Boyd and A. Ashkin, Phys. Rev. **146**, pp. 187, 1966.
16. D. A. Roberts, "Dispersion equations for nonlinear optical crystals: KDP, $AgGaSe_2$, and $AgGaS_2$," Appl. Opt. **35**, pp. 4677-4688, 1996.